The adsorption and XPS of triphenylamine-based organic dye molecules on rutile TiO_2(110) prepared by UHV-compatible electrospray deposition

Nouf Alharbi[1,2], Jack Hart[1] and James N. O'Shea[1]*

[1]*School of Physics & Astronomy, University of Nottingham, Nottingham, NG8 1ED, UK*

[2]*Department of Physics, Jazan University, Jazan 45142, Kingdom of Saudi Arabia*

**Corresponding author email:j.oshea@nottingham.ac.uk*

Abstract

We present an X-ray photoelectron spectroscopy (XPS) study of a series of organic triphenylamine-based organic dye molecules (D5, SC4 and R6) deposited onto an atomically clean TiO_2(110) single crystal surface by vacuum-compatible electrospray deposition. Coverages from sub-monolayer to few-layer are explored to determine the nature of the adsorption bond to the surface. In all three cases the dyes are found to anchor to the oxide surface via the deprotonation of the carboxylic group with little evidence of secondary bonding interactions. The XPS measurements show the intact deposition of the dyes onto the surface in a UHV environment facilitating the study of these model dye-sensitised solar cell systems using surface science techniques.

1. INTRODUCTION

For decades, renewable energy sources have received considerable global interest due to the increase in fossil fuel consumption. The abundant energy produced by the Sun and to a lesser extent indoor ambient lighting means that photovoltaic devices can play a large role in energy saving by being integrated into a variety of different surfaces. In some applications dye-sensitised solar cells (DSSCs) remain a promising complement to conventional silicon and thin film solar cells due to their transparency and tuneable colours, making them suitable for applications such as windows and glass facades [1–3]. The key components of a DSSCs device are a layer of semiconducting oxide material, commonly TiO_2, a photosensitiser, a redox-mediating electrolyte and a counter electrode. The dye molecules absorb photons and inject photoexcited electrons into the conduction band of the oxide to which they are chemisorbed.

Subsequently, these injected electrons are transported to transparent conducting oxide while the oxidised dye is reduced by transferring electrons from the redox mediating electrolyte.

Since their discovery two decades ago DSSCs have been largely dominated by organometallic dye complexes, typically based on rare transition metals such as ruthenium. More recently, organic dyes have become of great interest [4-11] due to features such as high molar extinction coefficients, low manufacturing costs, abundant elements (carbon, nitrogen, oxygen and sulphur) and ease of structural modification and synthesis [6]. The creation of dye aggregates on the surface of the semiconductor is one of the most significant issues contributing to the low conversion efficiency of organic dyes in DSSCs. To solve this problem and improve the light-harvesting efficiency, aggregation of dyes must be prevented to achieve the best performance, by increasing both the surface area of the semiconducting oxide and adsorption on the surface [12].

To understand the adsorption of organic dyes to metal oxide surfaces, X-ray photoelectron spectroscopy (XPS) provides an excellent probe of the chemical changes induced during the formation of the dye-surface chemisorption bonds. However, in very many cases, the dyes are large and fragile with the result that they cannot be thermally evaporated onto a surface in the ultra-high vacuum (UHV) environment required for many traditional surface science techniques. In recent years, *in-situ* electrospray deposition has enabled the application of core-level spectroscopies to the study of dye-sensitised oxide surfaces [13,14,15]. In this paper we present a thorough XPS investigation of the adsorption of three organic dye molecules D5, SC4 and R6, the structures of which are shown in figure 1, deposited onto single crystal rutile TiO_2(110) under near UHV conditions using *in-situ* electrospray deposition. These three dyes are all based around a triphenylamine moiety. One of the simplest dye molecules based on this structure is 4-(diphenylamino)phenylcyanoacrylic acid known as L0, we studied recently using core-level spectroscopy in the form of an *ex-situ* prepared sensitised photoelectrode. [16] The three related dyes studied here have applications in different colours of photoelectrode, perhaps the most interesting and complex being the blue dye “R6” which produced a blue DSSC with an efficiency of 12.6% [17].

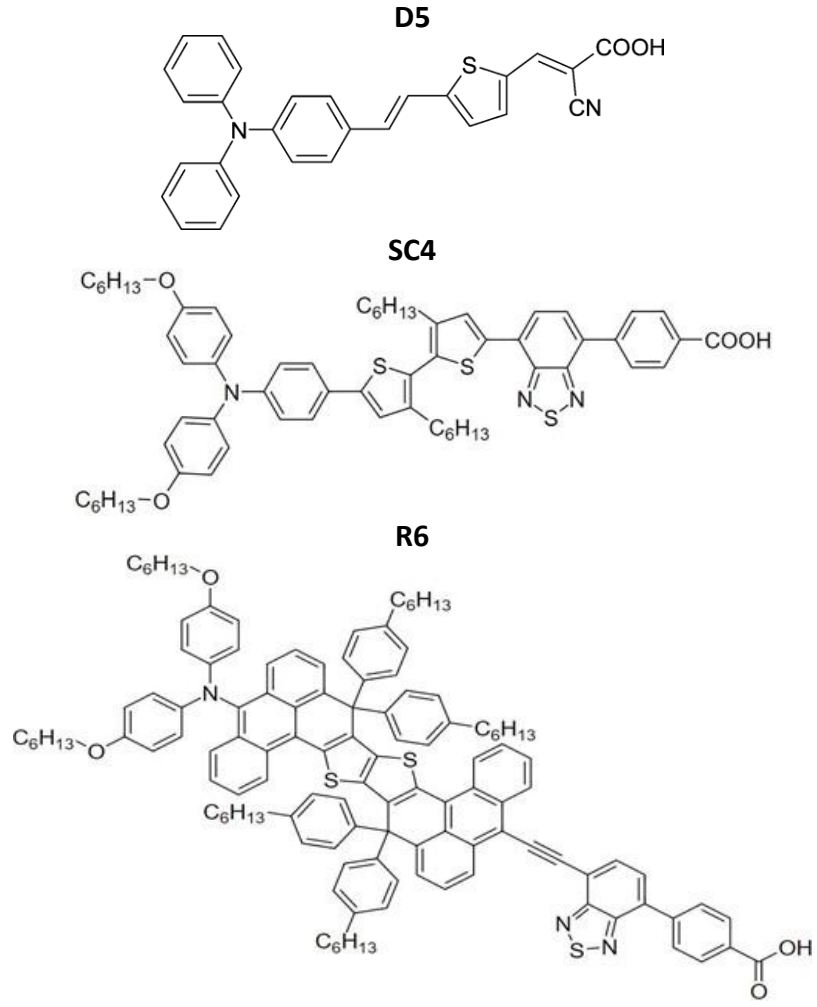

Figure 1. The molecular structures of D5, SC4 and R6 (full chemical names in the method section)

2. METHODS

The experiments were performed in a SPECS DeviSim NAP-XPS instrument consisting of an ultra-high vacuum (UHV) preparation/analysis chamber and interchangeable NAP cells that can be docked onto the entrance of the Phoibos 150 NAP hemispherical analyser. In this study all depositions and measurements were performed in the UHV analysis chamber with a base pressure in the 10^{-10} mbar range. A rutile TiO_2(110) crystal (PI-KEM Ltd.) was cleaned in UHV by rounds of 2 kV and 1 kV Ar^+ ion sputtering followed by annealing to 600°C until the Ti 2*p* XPS exhibited a single Ti^{4+} oxidation state and no signal was observed in the C 1*s* XPS.

A UHV-compatible electrospray deposition source (Molecularspray Ltd) was installed on the UHV preparation/analysis chamber and aligned such that the ion beam impinges on the sample in the same region as the XPS measurement to allow direct in-situ monitoring. The

source has three differential pumping stages and is described elsewhere [14,15,18]. The orange (λ_{max} 476nm) dye molecule known as D5 with the full name *3-(5-(4-(diphenylamino)styryl)thiophen-2-yl)-2-cyanoacrylic acid*, and the yellow (λ_{max} 456nm) dye known as SC4 with the full name *4-(7-(5'-(4-(bis(4-(hexyloxy)phenyl)amino)phenyl)-3,3'-dihexyl-[2,2'-bithiophen]-5-yl)benzo[c][1,2,5]thiadiazol-4-yl)benzoic acid* were dissolved in ethanol at an approximate concentration of 0.1 wt%. The blue (λ_{max} 631nm) dye molecule known as R6 with the full name *4-(7-((15-(Bis(4-(hexyloxy)phenyl)amino)-9,9,19,19-tetrakis(4-hexylphenyl)-9,19-dihydrobenzo[1',10']phenanthro[3',4':4,5]thieno[3,2-b]benzo[1,10]phenanthro[3,4-d]thiophen-5-yl)ethynyl)benzo[c][1,2,5]thiadiazol-4-yl)benzoic acid* was dissolved in tetrahydrofuran (THF) at approximately the same concentration (all dyes from Dyenamo AB). Dye solutions were electrosprayed from a tapered stainless-steel emitter with an OD360µm and ID100µm (NewObjective) at a constant flowrate delivered by a syringe pump at 0.3 ml/hr and an emitter voltage of +2.5kV. The electrospray system is separated from the preparation chamber by a UHV gate valve. With the valve open but no spray the pressure rises to the 10^{-8} mbar range and is in the low 10^{-6} mbar range during spraying, where the additional pressure is caused by residual solvent in the ion beam.

XPS data were measured at a pass energy of 20 eV excited by a monochromatic Al kα (1486.7 eV) photon energy and the binding energy scale calibrated to the Ti $2p_{3/2}$ peak of the stoichiometric TiO_2(110) substrate at 458.8 eV. A combination of a Shirley and linear background was removed from each spectrum before curve-fitting with 30% Lorentzian and 70% Gaussian combinations to approximate the Voigt lineshapes appropriate for the core-levels of organic molecules.

3. RESULTS AND DESICSION

3.1. D5 on TiO_2(110)

The structure of D5 is shown in Fig. 1. The electron donating triphenylamine group is located at the head of the molecule while the cyanoacetic acid group at the tail end acts as the acceptor and proposed anchoring ligand to the oxide surface. These are connected via a π-conjugated thiophene bridge. [11,19]

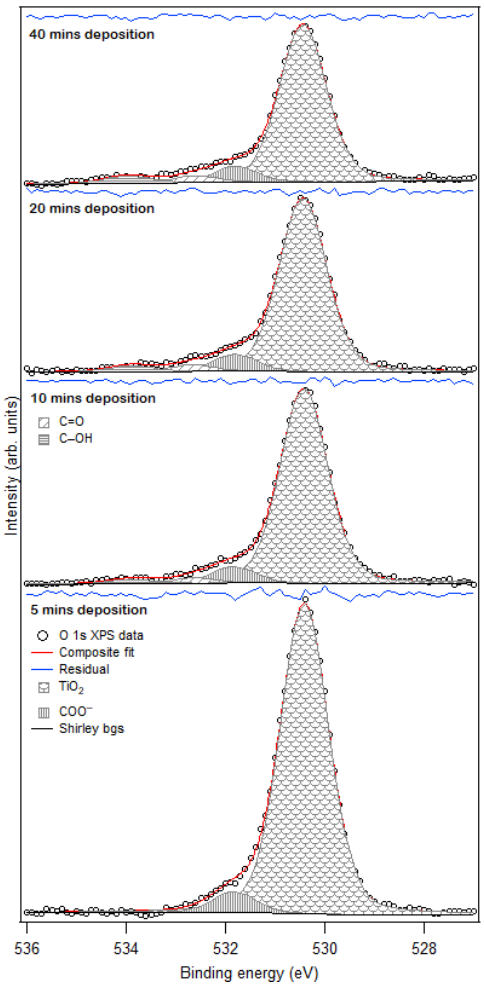

Figure 2. O 1*s* XPS as a function of electrospray deposition time for D5 on rutile TiO_2(110) showing a single peak from the molecule at low coverage due to the deprotonation of the carboxylic acid group.

The O 1*s* XPS for D5 depositions on the rutile TiO_2(110) surface ranging from 5 mins to 40 mins is shown in Fig. 2. The peak at 530.4 eV in all cases is attributed to TiO_2(110) substrate and dominates the spectra due to the large escape depth of the photoelectrons at the Al-kα photon energy. At 5 mins deposition, a single molecule peak is observed at 531.8 eV, which is assigned to COO^-. This is attributed to the deprotonation of the COOH group and the bonding of the O atoms to Ti atoms in the oxide surface. A similar adsorption geometry has previously been found for the related molecule 2-Cyano-3-(4-*N,N*-diphenylaminophenyl)-*trans*-acrylic acid thermally evaporated onto rutile TiO_2(110) [20] and is indeed a common feature of carboxylic acids on titanium dioxide [13,14]. As the coverage is increased, still a single molecule O 1*s* peak is observed after 10 mins deposition until at 20 mins two new peaks begin to emerge, becoming more intense at 40 mins deposition time. The molecule peak at 533.9

eV is assigned to O–H groups in non-deprotonated carboxyl groups, and the peak at 532.6 eV is assigned to the corresponding C=O group. In the isolated molecule we would therefore expect to observe a 1:1 ratio of these two new molecule peaks, while in the chemisorbed monolayer only a single peak due to the now equivalent oxygens in the deprotonated carboxyl group bound to surface titanium atoms should be observed. At both 20 mins and 40 mins an approximately 1:1 ratio is indeed observed in the experimental data. An additional consideration that does not impact the deduction of the deprotonation of the carboxylic anchoring group is that such a reaction should in principle lead to dissociated protons on the surface that could adsorb on the bridging oxygens to form surface OH groups. The results shown in Fig. 2 are not able to clarify the fate of the dissociated protons. Since we observe only one O 1*s* molecule peak at low coverage, the binding energy of the bridging OH likely overlaps in energy with the COO- peak at 531.8 eV, consistent with results from the adsorption of terephthalic acid on TiO_2(110) [21]. This would artificially increase the intensity of the peak at 531.8 eV, since the oxygen atom involved is contributed by the oxide substrate rather than the molecule. While not impacting the conclusion that the carboxylic acid is deprotonated (since this observation is based on the absence of the C-OH peak at 533.9 eV), this is a consideration for the quantification, and is revisited later in the context of the molecule R6.

The corresponding C 1*s* XPS for D5 is presented in Fig. 3. Considering first the lowest coverage (5 mins deposition), for which all molecules are chemisorbed to the surface (as shown by the O 1*s* spectra) the spectrum can be fitted to three components in the main peak and an additional peak to higher binding energy. The high energy peak at 288.7 eV is assigned to the deprotonated carboxylate group. The main contribution to the spectrum is the component at 285.3 eV, attributed to the aromatic carbons in the phenyl rings of the triphenylamine group and the backbone of the molecule. The component at 286.3 eV is therefore attributed to the carbon atoms bound to nitrogen in the triphenylamine and cyano group, while the component at 287.0 eV represents the thiophene moiety. We note that these latter two peak assignments are based on the relationship between the peak intensity and the stoichiometry within the molecule and that without supporting calculations these remain open to interpretation [16]. Nitrogen is more electronegative than sulphur but the triphenylamine carbons bound to the central nitrogen are in an aromatic ring, which may

counter this effect to some extent. In the molecule the components in the above order have a 1:21:4:2 ratio, which compares well to the 1:22:5:2 intensity ratio observed in Fig. 3, however we have deliberately not considered any shake-up features that may overlap with the peaks of the individual chemical groups as no information can be extracted from the data for these, although these could place an additional uncertainty on the peak ratios. For the simpler L0 molecule [16] shake-up features were observed at the higher energy of 290-292 eV because this falls outside of the window of the main photoemission peaks and renders them resolvable. Here no clear evidence of shake-up features are observed. For the slightly higher coverage at 40 mins deposition the same components are observed at the same binding energies within the uncertainty, with the exception of a possible upshift in energy of the peak now at 289 eV representing both carboxylate from the underlying monolayer and carboxylic acid in the partial second layer.

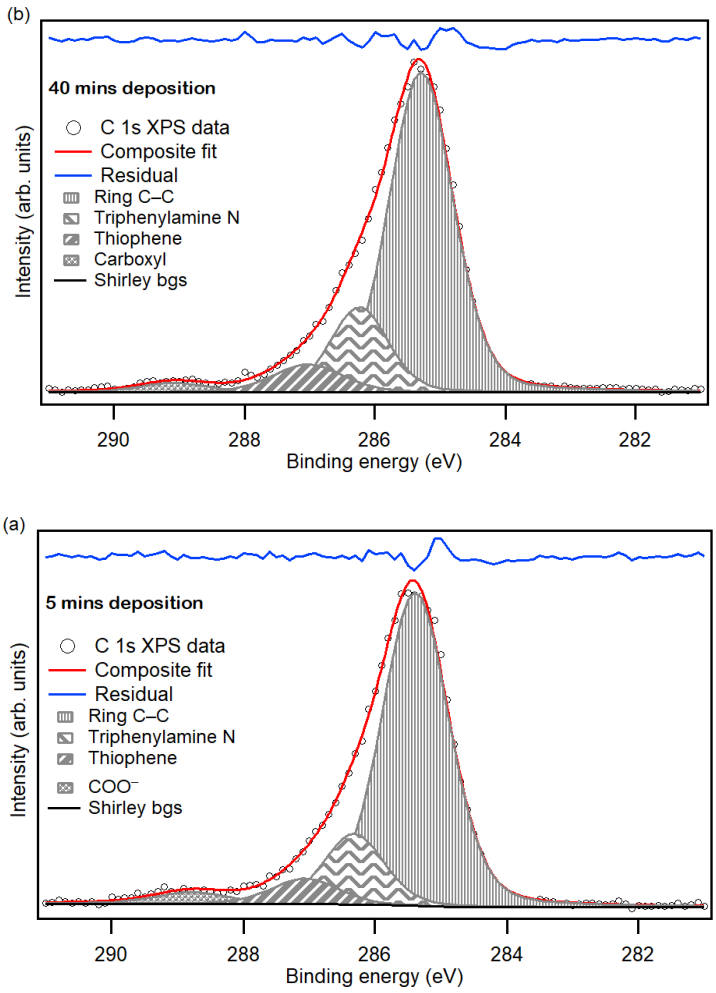

Figure 3. C 1*s* XPS as the lowest (sub-monolayer) and highest coverage (partial second layer) for D5 on the rutile TiO_2(110) surface.

Fig. 4 shows the corresponding N 1*s* XPS fitted with two components for all coverages (only lowest and highest shown). These are attributed to the nitrogen atoms in the triphenylamine (C–N) around 400.5 eV and nitrile (C ≡ N) at around 399.6 eV (within ±0.1 eV). Previous XPS observing the same moieties of triphenylamine and nitrile in L0, are consistent with these assignments [16]. Interestingly, the ratio of the two N 1*s* components is approximately 2:1 in both cases. This is also in agreement with previous results for L0 where the (C ≡ N) intensity is significantly lower, which has tentatively been attributed to shadowing of that end of the molecule due to the carboxylic acid being bound to the surface as suggested by the O 1*s* data [16]. It is worth noting that the overall coverage of D5 on the surface even after 40 mins deposition is still dominated by the monolayer and thus affected by the molecular orientation.

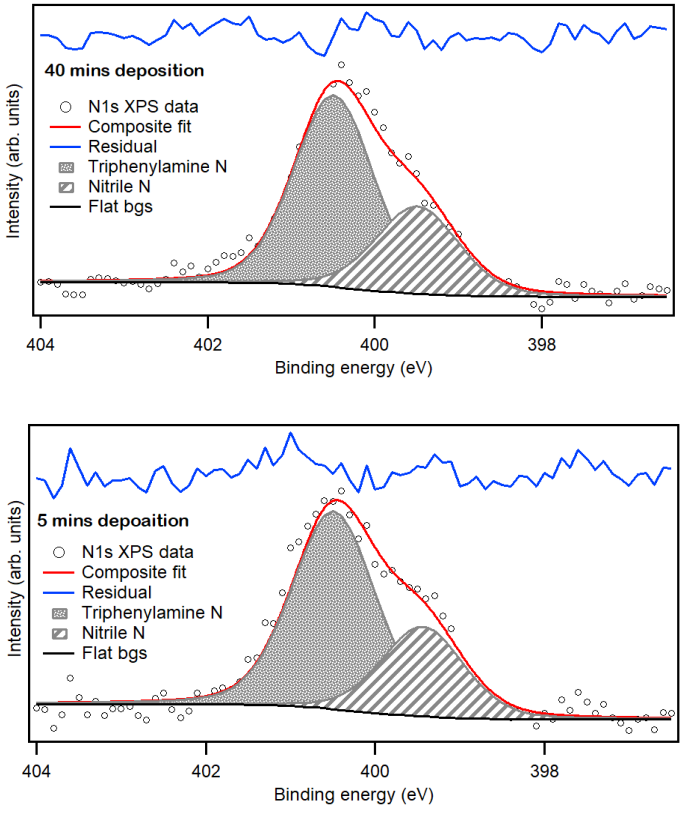

Figure 4. N 1*s* XPS as the lowest (sub-monolayer) and highest coverage (partial second layer) for D5 on the rutile TiO_2(110) surface. Both peaks have the same Lorentzian and Gaussian widths.

Fig. 5 shows the S 2*p* XPS for the 5 mins and 40 mins deposition surfaces, fitted with a single spin-orbit pair (splitting 1.2 eV and a branching ratio of 2:1) in both cases with a S $2p_{3/2}$ binding

energy of 164.8 eV, reflecting a single chemical environment of the sulphur atoms and suggesting that the sulphur atom is not interacting with the surface in the monolayer.

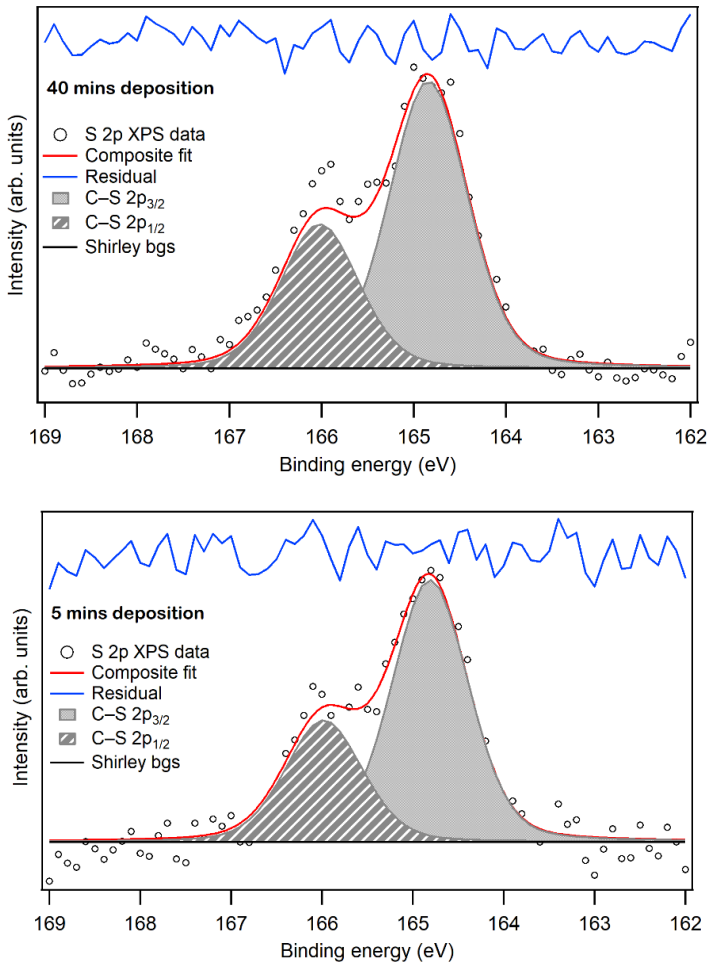

Figure 5. S 2*p* XPS as the lowest (sub-monolayer) and highest coverage (partial second layer) for D5 on the rutile TiO_2(110) surface.

A summary of the XPS energies is given in Table 1.

Table 1. A summary of the XPS component binding energies for D5 on the rutile TiO_2(110) surface.

		Peak BEs (eV)	
Core level		**5 mins**	**40 mins**
O 1*s*	TiO_2	530.4	530.4
	COO^-	531.8	531.8
	C=O		532.6
	C–OH		533.9
C 1*s*	Ring C–C	285.3	285.2
	Triphenylamine N	286.3	286.2
	Thiophene	287.0	287.0
	COO^-	288.7	289.0
N 1*s*	Triphenylamine N	400.4	400.4
	Nitrile N	399.4	399.4
S 2*p*	Thiophene	164.8	164.8

3.2. SC4 on TiO_2 (110)

SC4 has a similar chemical structure to D5 as shown in Fig. 1 but featuring a 4-(benzo[c][1,2,5]thiadiazol-4-yl)benzoic acid moiety as the acceptor/ anchor instead of the cyanoacetic acid of D5 [22]. SC4 also has some additional hexyloxy side chains to consider when interpreting the XPS.

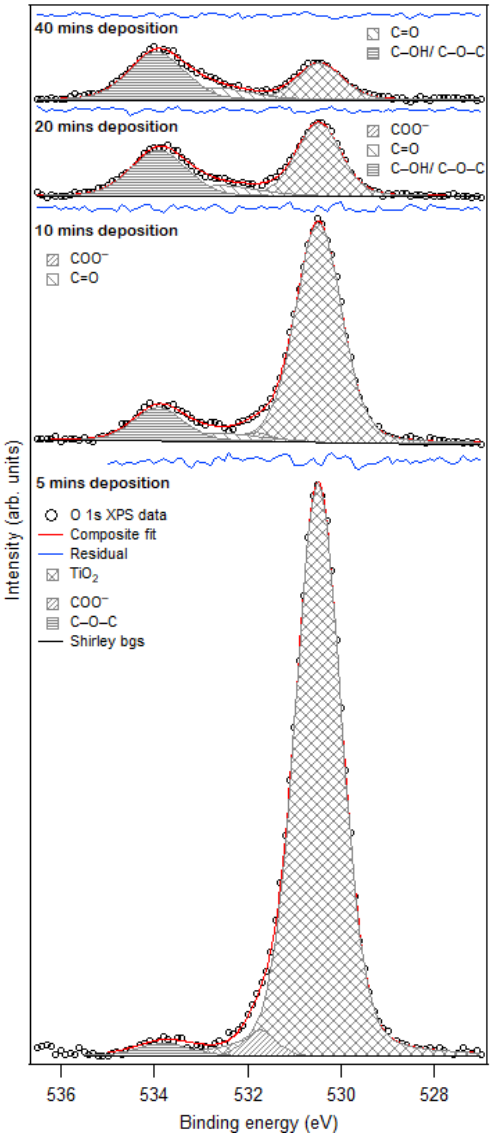

Figure 6. O 1*s* XPS as a function of electrospray deposition time for SC4 on rutile TiO_2(110).

Fig. 6 shows a comparison of the O 1*s* photoelectron spectra following increasing electrospray deposition times. If we consider first the 5 mins deposition the spectrum is dominated by the peak at 530.4 eV related to the underlying oxide substrate. To higher binding energy there is a resolvable peak at 533.9 eV which we can attribute to oxygen atoms singly bonded to carbon in the C-O-C moieties (which D5 does not have). This is also the binding energy at which we would expect to observe the C-OH of a non-deprotonated carboxylic acid group if present. Due to the intense substrate peak, the region in between is challenging to fit and we must turn to the highest coverage to have more confidence in this region. At 40 mins deposition time, we can observe a shoulder to the lower binding energy side of the C-O-C/C-O-H peak. This can be fitted with a component at 532.6 eV, which we can assign to the other oxygen atom in the isolated molecule, the C=O of the carboxyl group. At the highest coverage, where the oxide signal is strongly suppressed we can assume no deprotonation. The molecule O 1*s* is therefore fitted to two molecule components at 533.9 eV and 532.6 eV representing the C-O-C/C-O-H oxygens and the C=O oxygen. The ratio of the areas of these two components is 3:1, which agrees with the molecular stoichiometry (two C-O-C and one C-OH compared to one C=O). At the 5 mins deposition time however, no significant C=O peak can be fitted, reflecting the condition where the majority of the molecules are anchored to the surface via the deprotonated carboxyl group and the concomitant conversion of intensity from the C-O-H and C=O into COO- at which point we observe a 1:1 ratio of the C-O-C peak area (representing the two oxygens in that environment) to that of the COO- peak (with its two oxygens). However, we should consider the possibility that the peak at 531.8 eV could also have some contribution from bridging OH groups formed from the dissociated protons, thus in principle it would be possible to have an even lower ratio of 2:3 in the event of complete deprotonation (2 for C-O-C, 2 for COO- plus 1 for bridging OH). If the current lowest coverage (5 mins) does not represent complete deprotonation in line with this scenario, then we would include a small C=O peak in the fit too.

The C 1*s* XPS for SC4 is shown in Fig 7. Due to the number of different chemical environments within the SC4 molecule it would be prudent to consider the highest coverage first to minimize the effects of possible surface interactions. Considering the stoichiometry of the molecule the dominant contribution will be from aromatic carbons bound only to carbon, of which there are 29. Next most abundant, will be aliphatic carbons bound only to carbon, of

which there are 22, followed by aromatic carbons bound to nitrogen, of which there are 5. The remaining carbon atoms are the 4 bound to oxygen in the C-O-C groups, 4 bound to sulphur atoms in the thiophene bridge and finally 1 in the carboxylic acid. Based on the binding energy of the aromatic peak D5 we expect this to be located around 285.2 eV. At the other end of the spectrum, we would expect the carboxylic peak around 289 eV but is vanishingly weak in comparison to the others. Based on literature values for the separation between aliphatic and aromatic carbons in a molecule containing both we have placed the aliphatic peak 0.6 eV to higher binding energy around 285.8 eV [23]. Based on our D5 fit, we expect the thiophene peak at around 287.0 eV and for the carbon bound to N we could reasonably expect to observe at 286.3 eV.

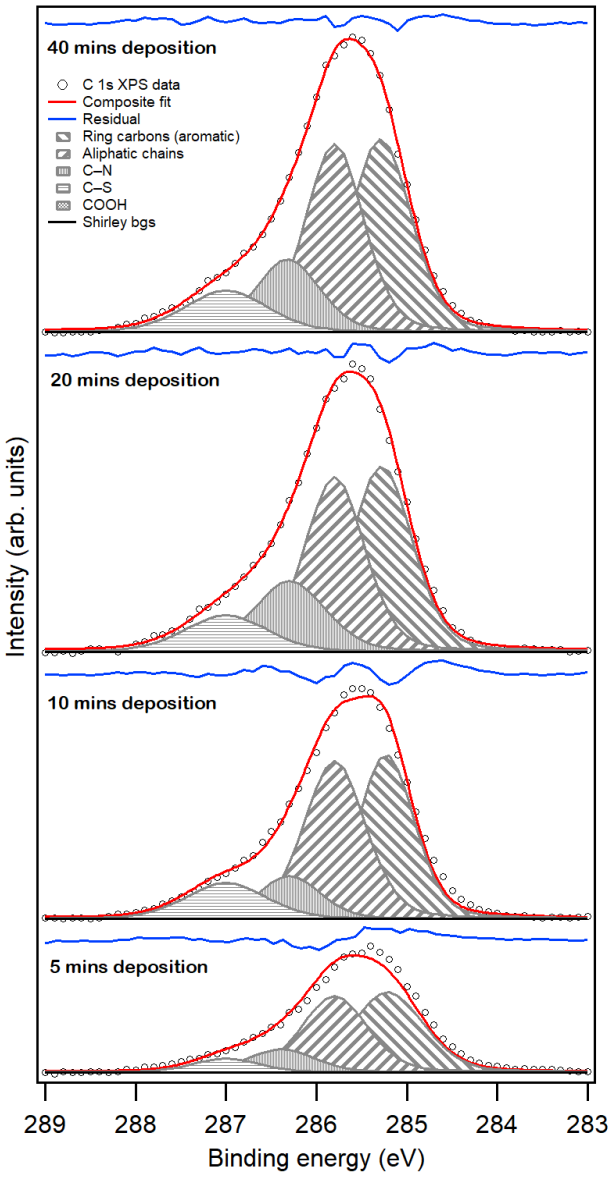

Figure 7. C 1*s* XPS as a function of electrospray deposition time for SC4 on rutile TiO_2(110).

The corresponding N 1*s* XPS for SC4 is shown in Fig. 8. SC4 has one nitrogen atom in the triphenylamine (C–N) ligand and two bound to sulphur (N–S) in the thiophene bridge. Despite these two different chemical environments the spectrum exhibits just one peak at 400.4 eV. The width of this peak is 1.1 eV (±0.1 eV) is the same as each of the two components fitted for D5 previously. This single peak is attributed to a coincidence in the binding energy within our resolution of these two states. A slight downward shift in binding energy is observed for the lowest coverage similar to that observed in the O 1*s*, due to increased screening from the oxide substrate.

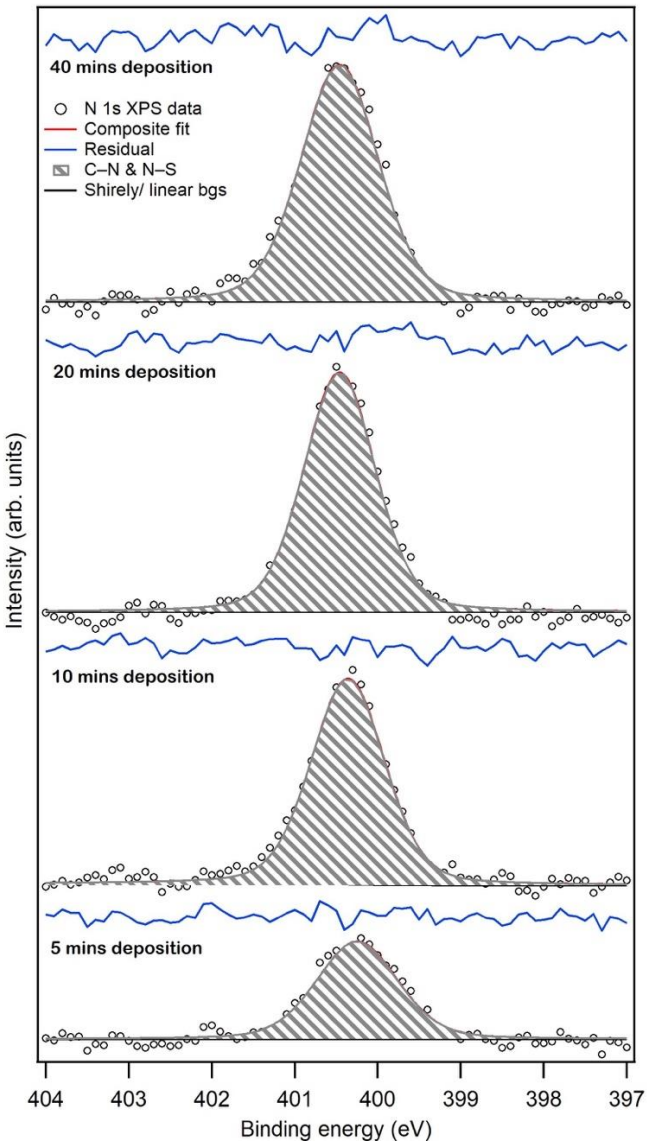

Figure 8. N 1*s* XPS as a function of electrospray deposition time for SC4 on rutile TiO_2(110).

The S 2*p* XPS for SC4 is shown in Fig. 9 where two distinct spin-orbit split doublets are observed with S $2p_{3/2}$ binding energies at 164.5 eV and 166.1 eV for the highest coverage. These are attributed to sulphur bonded to carbon, and sulphur bonded to nitrogen respectively. The ratio of the intensities of these two states is approximately 2:1 for all coverages, as expected from the sulphur atomic ratio in the molecule, with just a small shift to lower binding energy for the lowest coverage. A summary of the XPS energies is given in Table 2.

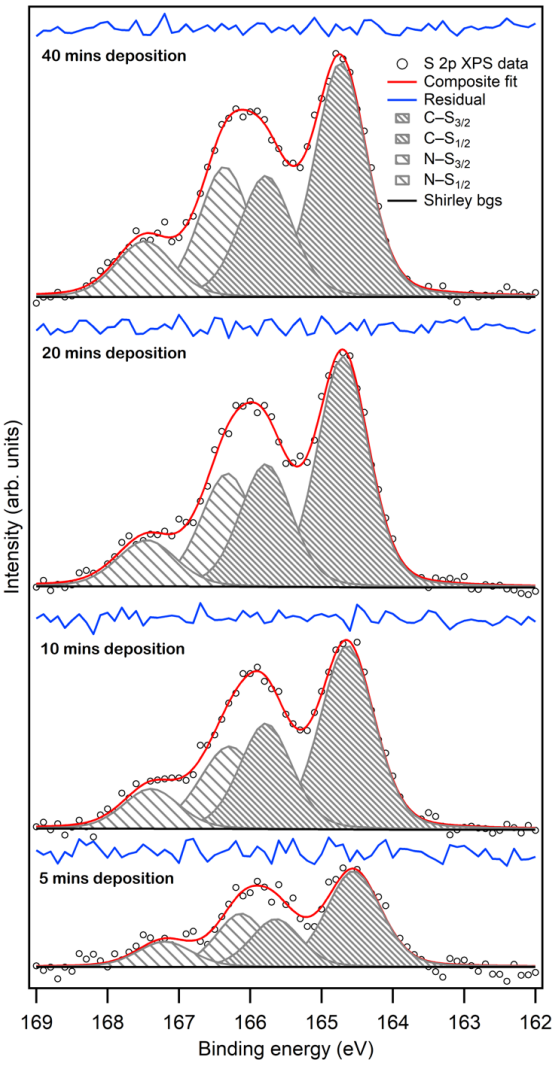

Figure 9. S 2*p* XPS as a function of electrospray deposition time for SC4 on rutile TiO_2(110).

Table 2. A summary of the XPS component binding energies for SC4 on the rutile TiO_2(110) surface.

		Peak BEs (eV)	
Core level		**5 mins**	**40 mins**
O 1*s*	TiO_2	530.4	530.4
	COO^-	531.8	
	C=O		532.6
	C–OH & C–O–C	533.9	533.9
C 1*s*	Ring C–C	285.2	285.2
	Aliphatic C–C	285.8	285.8
	Triphenylamine	286.3	286.3
	Thiophene	287.0	287.0
	Carboxyl C	289.0	289.0
N 1*s*	Triphenylamine N & N–S	400.2	400.4
S 2*p*	C–S	164.5	164.7
	N–S	166.1	166.3

3.3. R6 on TiO_2 (110)

The structure of R6 is shown in Fig. 1. This blue dye has a far more complex backbone than SC4 but essentially no new motifs have been introduced in terms of the interpretation of the XPS. The acceptor and anchoring ligand remains a 4-(benzo[c][1,2,5]thiadiazol-4-yl)benzoic acid moiety [17, 24, 25]. Chemisorption of the R6 dye to the TiO_2(110) surface is therefore expected to result in deprotonation of the carboxylic acid group to form a 2M-bidentate anchor as for D5 and SC4.

Fig. 10 displays the O 1*s* XPS for electrospray deposition times of 10, 20 and 40 mins (5 not shown as the molecule contribution to the spectra is too weak). The dominant peak at 530.4 eV is assigned to the oxide surface in all coverages as for the previous molecules. Considering first the highest coverage (40 mins) it becomes apparent that fitting parameters cannot be translated directly from SC4 to R6 despite the similarity in the constituent groups. A satisfactory fit is only obtain for each coverage if the peak assigned to C-O-C is shifted to lower binding energy than in SC4, now located 0.6 eV lower in binding energy at 533.3 eV. The reason for this shift is unclear, but may be related to the larger aromatic backbone of the R6 molecule compared to SC4 which could encourage the molecule to lie flatter on the surface offering some screening of the C-O-C groups. As in SC4, the carboxylic acid group has contributions at 533.9 eV and 532.6 eV for the C-OH and C=O components respectively. Also consistent with SC4 and D5 is the peak at 531.8 eV attributed to COO^-. In the absence of deprotonation of the carboxylic group in the isolated molecule, we would expect a ratio of

1:2:1 for the C-OH, C-O-C and C=O peaks and no peak at 531.8 eV. At 40 mins the observed ratio is 1:4:1 with a small peak at 531.8 eV consistent with the contribution from the deprotonated chemisorbed monolayer. As the coverage decreases at 20 mins, the contribution from C-OH at 533.9 eV and C=O at 532.6 eV is almost negligible reflecting a larger proportion of deprotonated molecules on the surface and a ratio of the C-O-C:COO- peaks of approximately 1:1. For the 10 mins deposition the ratio of C-O-C:COO- is lower than the expected minimum of 1:1 and approaches 2:3. This scenario was briefly discussed in the context of SC4 and tentatively attributed to the formation of bridging OH groups with a binding energy that overlaps that of the COO- species. Further studies are required to find the minimum ratio of these peaks to confirm this hypothesis.

In Fig. 11 we present the C 1*s* XPS as a function of electrospray deposition times. The assignments of the carbon components should in principle be approximately the same as for SC4 with only the relative intensities changing as a result of the different number of carbon atoms in each environment. Considering first the highest coverage spectrum. This has been fitted to a series of components at 285.0, 285.5, 286.1, 286.8 and 289.0 eV representing the aromatic carbons (of which there are 89), aliphatic carbons (of which there are 36), carbon-nitrogen (of which there are 5), thiophene (of which there are 4) and carboxylic (a single carbon).

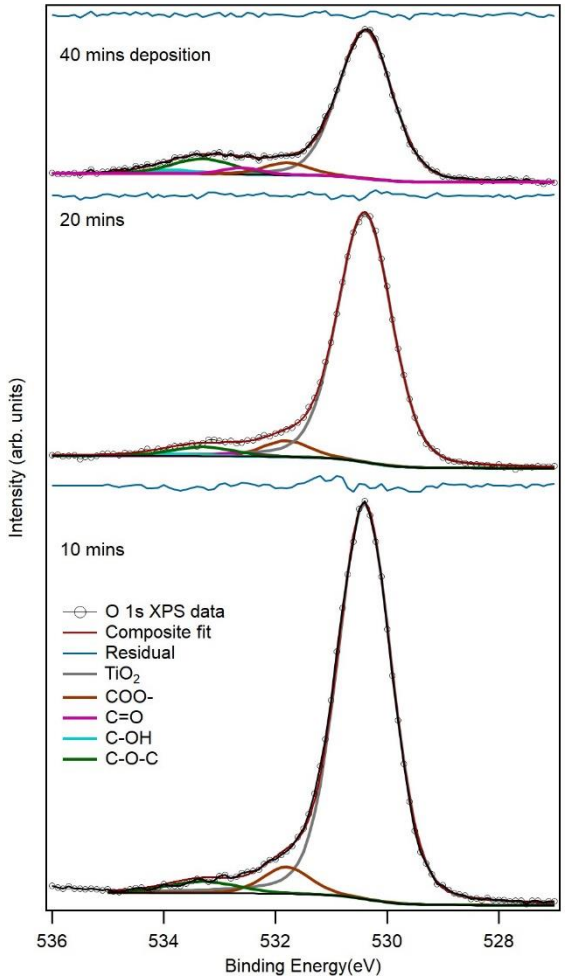

Figure 10. O 1*s* XPS as a function of electrospray deposition time for R6 on rutile TiO_2(110) showing deprotonation of the carboxylic group for the first absorbed monolayer.

The expected ratio based on the stoichiometry is therefore 89:36:5:4:1 which is consistent with the intensity ratios observed in Fig. 11. These ratios do not change significantly as a function of surface coverage, consistent with the observation that the interaction with the surface is through the carboxylic group only and not involving bond formation with other parts of the molecule.

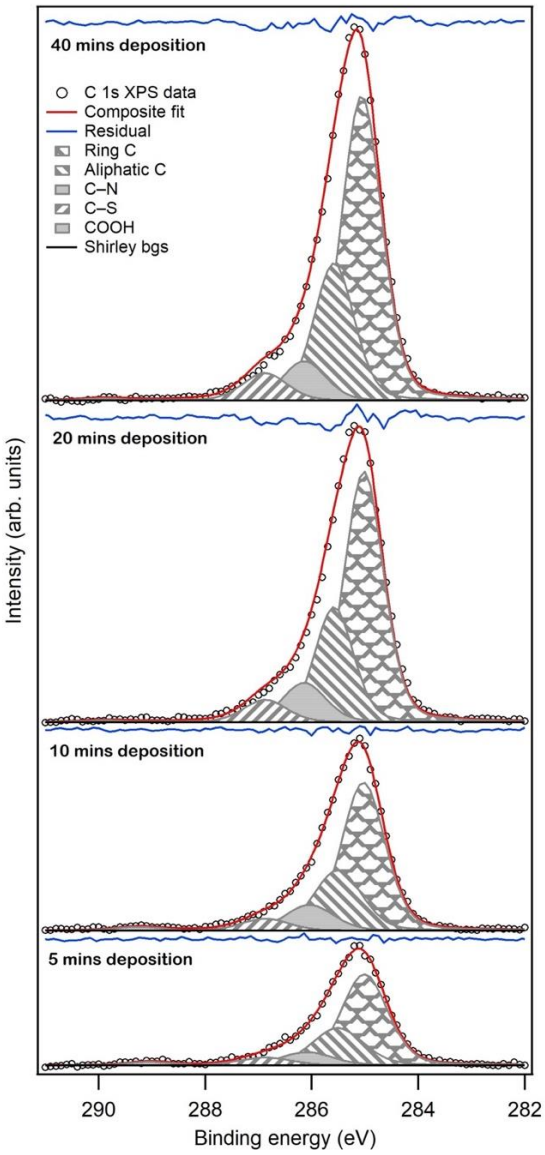

328

329 **Figure 11.** C 1*s* XPS as a function of electrospray deposition time for R6 on rutile TiO_2(110).

330

331 The N 1*s* XPS is shown in figure 12 for the highest and lowest coverage of R6 on the TiO_2(110)
332 surface. As observed also for SC4, for all coverages (not shown) the C–N and N–S moieties
333 exhibit a single peak, as a result of the coincidence in their binding energies at 400.1 eV.

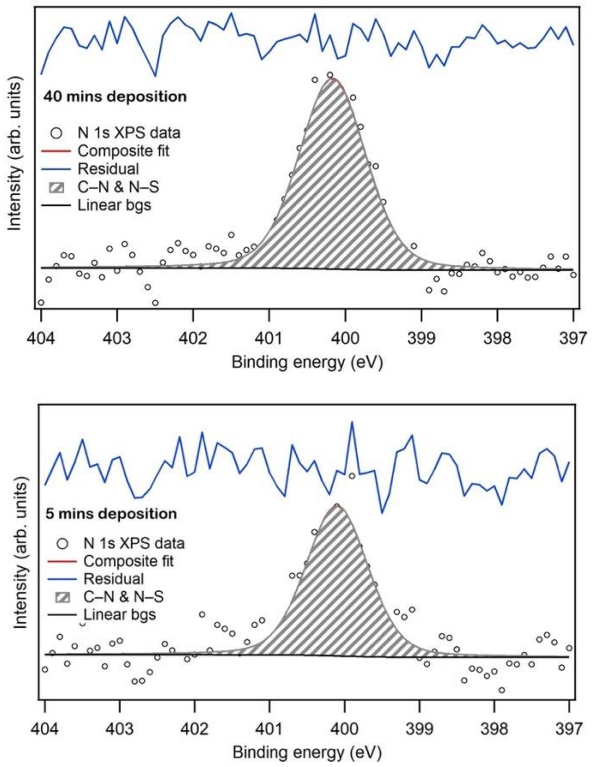

Figure 12. N 1*s* XPS as a function of electrospray deposition time for R6 on rutile TiO_2(110).

The environments of the sulphur atoms in R6 are identical to those in SC4 in the form of two C-S-C environments and one N-S-N environment. Two chemical environments are observed at both the lowest and highest coverage in the S 2*p* XPS in Fig. 13. The low binding energy doublet is again assigned to the C-S bond while the higher energy doublet corresponds to the N-S bond. The relative intensity ratio of the two doublets reflects the 2:1 ratio of these environments in the molecule. At the lowest coverage the intensity of the N-S environment is slightly reduced, most likely due to this state being closer to the end of the molecule that is anchored to the surface and therefore deeper into the molecule from the point of view of the escape depth of the photoelectrons. A summary of the XPS energies is given in Table 3.

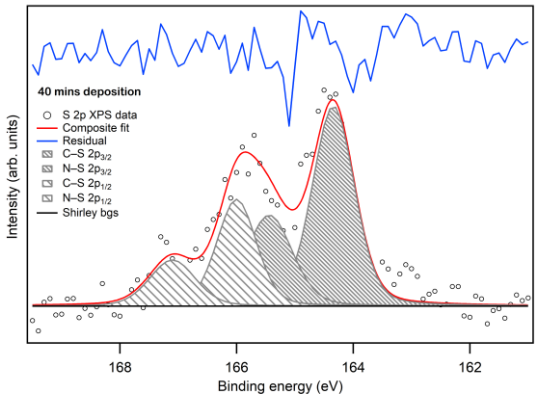

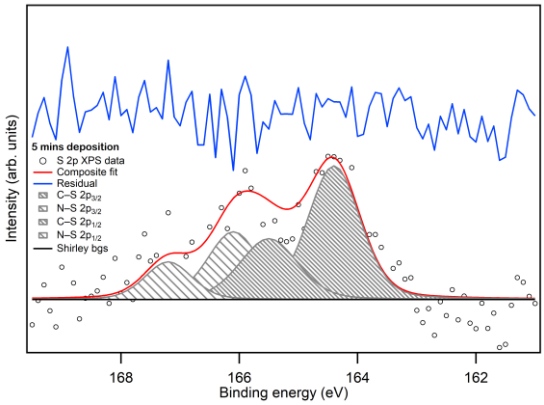

Figure 13. S 2*p* XPS for the highest (40 mins) and lowest coverage (5 mins) of R6 on rutile TiO_2(110).

Table 3. A summary of the XPS component binding energies for R6 on the rutile TiO_2(110) surface.

		Peak BEs (eV)	
Core level		**Low coverage**	**High coverage**
O 1*s*	TiO_2	530.4	530.4
	COO^-	531.8	531.8
	C=O		532.6
	C–O–C	533.3	533.3
	C–OH		533.9
C 1*s*	Ring C–C	285.0	285.0
	Aliphatic C–C	285.5	285.5
	Triphenylamine	286.0	286.1
	Thiophene	286.8	286.8
	Carboxyl C	289.0	289.0
N 1*s*	Triphenylamine N & N–S	400.1	400.1
S 2*p*	C–S	164.4	164.3
	N–S	166.1	166.0

4. Conclusions

A series of triphenylamine organic dye molecules of increasing complexity (D5 – SC4 – R6) have been deposited onto a single crystal rutile TiO_2(110) surface using UHV-compatible electrospray deposition. XPS measurements have been made as a function of electrospray deposition time to investigate how the chemical environments of the functional groups of the dye molecules vary as a function of coverage. In all cases the XPS is consistent with the intact adsorption on the surface with the only significant interaction being the deprotonation of the carboxylic acid group at the acceptor/anchoring end of the molecule. This is consistent with the expectation that the acceptor end of the dye to which the photoexcited electrons in a dye sensitised solar cell are shuttled for efficient tunnelling into the conduction band of the oxide substrate. That no interactions between other parts of the molecule and the surface were observed and the suppression of the photoemission signal from the anchoring end supports a picture in which the dye molecules are broadly upright on the surface in the monolayer. This is also beneficial in terms of a DSSC as the donor end of the molecule is located away from the surface for efficient photoexcitation and replenishment of the lost electron through interaction via a redox electrolyte. Further investigation using near-edge X-ray absorption fine structure (NEXAFS) with linearly polarised soft X-rays is required to confirm the orientation of the molecules on the surface and would also benefit from scanning tunnelling microscopy (STM). The in-situ deposition of these complex non-volatile dye molecules onto surfaces prepared under UHV conditions enables these further investigations including an exploration of the charge transfer dynamics using resonant core-level spectroscopies.

Acknowledgments

JNO and JH acknowledge and thank Innovate UK through the Energy Research Accelerator, the Engineering and Physical Sciences Research Council (EPSRC) through the Fuel Cells and Their Fuels Centre for Doctoral Training (CDT), and the University of Nottingham Propulsion Futures Beacon for funding this research. NA acknowledges the Saudi Arabian Cultural Bureau and Jazan University for scholarship funding. The authors also acknowledge Filipe Louly Quinan Junqueira (University of Nottingham) for producing the graphical abstract.

386

387 **References**

388 [1] B. O'Regan and M. Grätzel, A low-cost, high-efficiency solar cell based on dye-sensitized
389 colloidal TiO_2 films. *Nature*, 353(6346):737–740, 1991.

390 [2] M. Grätzel, Recent advances in sensitized mesoscopic solar cells. *Accounts of Chemical*
391 *Research*, 42(11):1788–1798, 2009.

392 [3] A. Hagfeldt and M. Grätzel, Light-induced redox reactions in nanocrystallin systems.
393 *Chemical Reviews*, 95(1):49–68, 1995.

394 [4] M. Chandrasekharam, B. Chiranjeevi, K. S. V. Gupta, S. P. Singh, A. Islam, L. Han, and M. L.
395 Kantam, Simple Metal-Free Organic D-π-A Dyes with Alkoxy-or Fluorine Substitutions:
396 Application in Dye Sensitized Solar Cells. *Journal of Nanoscience and Nanotechnology*,
397 12(6):4489–4494, 2012.

398 [5] A. Mishra, M. K. R. Fischer, and P. Bàuerle, Metal-free organic dyes for dye sensitized solar
399 cells: From structure: Property relationships to design rules. *Angewandte Chemie*
400 *International Edition*, 48(14):2474–2499, 2009.

401 [6] K. M. Karlsson, X. Jiang, S. K. Eriksson, E. Gabrielsson, H. Rensmo, A. Hagfeldt, and L. Sun,
402 Phenoxazine dyes for dye-sensitized solar cells: relationship between molecular structure and
403 electron lifetime. *Chemistry–A European Journal*, 17(23):6415–6424, 2011.

404 [7] D. P. Hagberg, J-H. Yum, H. Lee, F. De Angelis, T. Marinado, K. M. Karlsson, R. Humphry-
405 Baker, L. Sun, A. Hagfeldt, M. Grätzel, et al. Molecular engineering of organic sensitizers for
406 dye-sensitized solar cell Applications, *Journal of the American Chemical Society*,
407 130(19):6259–6266, 2008.

408 [8] K. Hara, T. Sato, R. Katoh, A. Furube, Y. Ohga, A. Shinpo, S. Suga, K. Sayama, H. Sugihara,
409 and H. Arakawa. Molecular design of coumarin dyes for efficient dye- sensitized solar cells.
410 *The Journal of Physical Chemistry B*, 107(2):597–606, 2003.

411 [9] T. Horiuchi, H. Miura, K. Sumioka, and S. Uchida. High efficiency of dye-sensitized solar
412 cells based on metal-free indoline dyes. *Journal of the American Chemical Society*,
413 126(39):12218–12219, 2004.

[10] S. Kim, J. K. Lee, S. O. Kang, J. Ko, J-H. Yum, S. Fantacci, F. De Angelis, D. Di Censo, Md. K. Nazeeruddin, and M. Grätzel. Molecular engineering of organic sensitizers for solar cell applications. *Journal of the American Chemical Society*, 128(51):16701– 16707, 2006.

[11] D. P. Hagberg, T. Edvinsson, T. Marinado, G. Boschloo, A. Hagfeldt, and L. Sun. A novel organic chromophore for dye- sensitized nanostructured solar cells. *Chemical Communications*, (21):2245– 2247, 2006.

[12] G. Di Carlo, D. Caschera, R. G. Toro, C. Riccucci, G. M. Ingo, G. Padeletti, L. De Marco, G. Gigli, G. Pennesi, G. Zanotti, et al. Spectroscopic and morphological studies of metal-organic and metal-free dyes onto titania films for dye-sensitized solar cells. *International Journal of Photoenergy*, 2013, 2013.

[13] L. C. Mayor, J. Ben Taylor, G. Magnano, A. Rienzo, C. J. Satterley,

J. N. O'Shea, and J. Schnadt. Photoemission, resonant photoemission, and X-ray absorption of a Ru (II) complex adsorbed on rutile TiO_2 (110) prepared by in situ electrospray deposition. *The Journal of chemical physics*, 129(11):114701, 2008.

[14] M. Weston, A. J. Britton, J. N. O'Shea, Charge transfer dynamics of model charge transfer centers of a multicenter water splitting dye complex on rutile TiO_2(110), *Journal of chemical physics 134 (5), 054705*

[15] A. J. Gibson, R. H. Temperton, K. Handrup, M. Weston, L. C. Mayor, J. N. O'Shea, Charge transfer from an adsorbed ruthenium-based photosensitizer through an ultra-thin aluminium oxide layer and into a metallic substrate, *The Journal of Chemical Physics 140 (23), 234708*

[16] R. H. Temperton, J. Hart, N. Verykokkos, E. Gibson, J. N. O'Shea, A soft x-ray probe of a titania photoelectrode sensitized with a triphenylamine dye, *The Journal of Chemical Physics 154 (23), 234707*

[17] Y. Ren, D. Sun, Y. Cao, H. N. Tsao, Y. Yuan, S. M Zakeeruddin, P. Wang, and M. Grätzel, A stable blue photosensitizer for color palette of dye-sensitized solar cells reaching 12.6% efficiency. *Journal of the American Chemical Society*, 140(7):2405–2408, 2018.

[18] R. H. Temperton, J. N. O'Shea, D. J. Scurr, On the suitability of high vacuum electrospray deposition for the fabrication of molecular electronic devices, Chemical Physics Letters 682, 15-19, 2017

[19] E. M. J. Johansson, T. Edvinsson, M. Odelius, D. P Hagberg, L. Sun, A. Hagfeldt, H. Siegbahn, and Hakan Rensmo. Electronic and molecular surface structure of a polyene-diphenylaniline dye adsorbed from solution onto nanoporous TiO_2, *The Journal of Physical Chemistry C*, 111(24):8580–8586, 2007.

[20] S. Yu, S. Ahmadi, M. Zuleta, H. Tian, K. Schulte, A. Pietzsch, F. Hennies, J. Weissenrieder, X. Yang, and M. Göthelid. Adsorption geometry, molecular interaction, and charge transfer of triphenylamine-based dye on rutile TiO_2 (110). *The Journal of chemical physics*, 133(22):224704, 2010.

[21] W. Zhang, L. Cao, L. Wan, L. Liu, F. Xu, A Photoelectron Spectroscopy Study on the Interfacial Chemistry and Electronic Structure of Terephthalic Acid Adsorption on TiO_2(110)-(1×1) Surface, *J. Phys. Chem. C* 2013, 117, 41, 21351–21358

[22] S. Chen, L. Yang, J. Zhang, Y. Yuan, X. Dong, and P. Wang. Excited-state and charge Carrier dynamics in a high-photovoltage and thermostable dye-sensitized solar cell. *ACS Photonics*, 4(1):165–173, 2017.

[23] A. Rienzo, L. C. Mayor, G. Magnano, C. J. Satterley, E. Ataman, J. Schnadt, K. Schulte, and J. N. O'Shea. X-ray absorption and photoemission spectroscopy of zinc protoporphyrin adsorbed on rutile TiO_2 (110) prepared by in situ electrospray deposition. *The Journal of chemical physics*, 132(8):084703, 2010.

[24] P. K. Samanta and N. J English. Opto-electronic properties of stable blue photosensitisers on a TiO_2 anatase-101 surface for efficient dye- sensitised solar cells, *Chemical Physics Letters*, 731:136624, 2019.

[25] G. Boschloo. Improving the performance of dye-sensitized solar cells. *Frontiers in Chemistry*, 7:77, 2019.